NEW ZEALAND JOURNAL OF ECOLOGY

RESEARCH

A spatial layer of human terrestrial pressures for New Zealand

Olivia R. Burge[1]*, Richard Law[2] and Sandy Wakefield[3]

[1]Manaaki Whenua – Landcare Research, PO Box 69040, Lincoln 7640, New Zealand
[2]Manaaki Whenua – Landcare Research, Private Bag 11052, Palmerston North 4442, New Zealand
[3]Centre for Integrative Ecology, School of Biological Sciences, University of Canterbury, Private Bag 4800, Christchurch 8140, New Zealand
*Author for correspondence (Email: burgeo@landcareresearch.co.nz)

Published online: 21 January 2025

Abstract: The global Human Footprint Map is a measure of human pressures on the environment that has been linked to changes in species extinction risks and the loss of intact ecosystems. Previous work assessed the utility of downscaling the global map to more precise regional scales using a 90 m resolution, and found that doing so supported conservation-based land-use planning. We created a New Zealand human pressure layer in a resolution (100 m) and projection (New Zealand Transverse Mercator 2000) suitable for national-scale analysis for the years 2012 and 2018. We used locally appropriate data sources for the global pressures (built environment, cropland, navigable waterways, pasture, population density, rail, road, visible nightlights). We found our pressure layer, and the underlying individual layers, to be useful for understanding (a) pressures on protected land ranked according to an international schema, and (b) how pressures around wetlands in 2012, particularly pressures relating to pasture and roads, differentiate wetlands that were lost between 2012 and 2018 from those that remained extant during this period.

Keywords: human footprint, protected land, spatial layers, wetlands

Introduction

Global measures of human pressures (introduced as the Human Footprint Map; Sanderson et al. 2002) have been developed and linked to the ongoing loss of intact ecosystems. Such maps are created using geospatial data that represent key anthropogenic pressures on natural ecosystems, such as transport corridors and human settlements. As such, they are useful for describing the spatial distribution of anthropogenically driven environmental pressures on ecosystems. In 2002 the first global Human Footprint Map was released, nominally timestamped 1993 (Sanderson et al. 2002). The first time series was created for the years 1993 and 2009 (Venter et al. 2016a), and this was later extended to cover the years 2000, 2005, 2010, and 2013 (Williams et al. 2020). Mu et al. (2022) extended the methodology (particularly by creating a time-sequence of nightlight visibility) to create a set of annual human pressure maps from 2000 to 2018. Applications of the pressure layers include the first layer in 2002 revealing that 83% of the earth was directly affected by humans (Sanderson et al. 2002); and work by Williams et al. (2020) who linked increases in human pressure to losses of intact ecosystems. Other applications of the human pressure layers include linking changes in the human footprint (i.e. human pressures) to changes in species extinction risks (Di Marco et al. 2018); while Woolmer et al. (2008) assessed the utility of downscaling (moving from a coarse to a fine spatial resolution) the methodology to regional scales using a 90 m resolution and using regionally specific component pressure layers, and found that doing so supported conservation-based land-use planning.

There is great potential for a human pressure layer[1] to assist with conservation planning and research in New Zealand. At present, abiotic and climate variables are well served (e.g. McCarthy et al. 2021), and land cover is available (MWLR 2020a), but a human pressure layer does not exist in a readily available format. Potential applications of a human pressure layer in New Zealand include improving species distribution models that use climate and other abiotic factors to predict ideal restoration sites within New Zealand by constraining them to avoid high-pressure areas. Land cover data could be combined with a human pressure layer to predict potential areas of anthropogenic impact on threatened ecosystems; this could assist with prioritisation of monitoring and conservation efforts, for example, within lowland indigenous forest remnants. A national human pressure layer could also be used to control for pressures on restoration projects where success and failure rates are compared; previous work has indicated that bias in starting condition confounds an assessment of whether passive or active restoration is more successful (Reid et al. 2018).

The global Human Footprint Map is unsuitable for use at the national scale in New Zealand. The global layer uses a

[1]Venter et al. (2016a) ask that "Human Footprint Map" only be used to refer to the data layers they created; therefore we refer to 'pressure layers' in this manuscript unless referring to the Venter et al. (2016a) data.

DOI: https://doi.org/10.20417/nzjecol.49.3580

1 km resolution, which is appropriate for its global extent, and also uses the Mollweide projection. Although the Mollweide projection is well suited for representing global distributions, it compromises representations of angle and shape to preserve area, resulting in severe distortions for map representations over New Zealand and other mid-latitude regions. In contrast, Transverse Mercator projections are better suited for depicting elongated areas in a north–south direction, and the New Zealand Transverse Mercator (NZTM) also minimises distortion in the east–west extents. New Zealand Transverse Mercator is a popular map projection for depicting New Zealand and is used for official topographic maps produced in New Zealand. This makes the NZTM suitable for national analysis for New Zealand, and for integrating other data available in the same projection. As such, we saw potential to improve the applicability of the global layer by creating two timestamped layers (2012 and 2018) that:

(1) use locally appropriate data sources: specifically, we used national datasets of land cover, roads, railways, rivers, and coastlines to address published concerns about the quality of global data in terms of accuracy, completeness, and resolution (Woolmer et al. 2008);

(2) increase the resolution of the layer to 100 m, as many national-scale datasets use a 100 m resolution, such as the New Zealand Environmental Data Stack (McCarthy et al. 2021);

(3) adopt the NZTM projection to also allow for easier integration with other New Zealand data already in the NZTM.

The global layer has had its applicability tested and validated using a set of satellite images that were manually scored for visual indications of human disturbance (Venter et al. 2016b; Mu et al. 2022). The global method was applied for the New Zealand version, so we do not repeat this validation exercise here. Instead, to inform potential users, we assess where and why the New Zealand version differs from the global version (as in Mu et al.; 2022).

We also assess the utility of the local layer by using it to address two questions: (1) do categories of New Zealand's protected land, as ranked by the International Union for Conservation of Nature (IUCN) protection criteria (Bellingham et al. 2016), correlate with human pressure scores (2018) for that land?; and (2) do human pressure scores in 2012 for a 100 m buffer around wetlands correlate with subsequent wetland loss or retention in 2018? This latter question is based on work that suggests incremental disturbance may occur before a wetland is entirely lost (Robertson et al. 2019).

Wetland conservation and loss are critical in the face of the increasing frequency of extreme climate events and the services wetlands provide in terms of flood mitigation (Clarkson et al. 2013; Patterson & Cole 2013). We chose a 100 m buffer because recent policy (New Zealand's National Policy Statement for Freshwater Management 2020, and policy promulgated from it) restricts the establishment of earthworks, including new drains, within 100 m of wetlands; it does not affect existing drains. One hundred metres is also conservative with respect to the documented ecological edge effects of drains, which are reviewed in Burge et al. (2023).

Methods

As an overview, we followed the approach of the global methodology, combining eight key anthropogenic pressures into one combined pressure layer. The pressures were: roads, railways, built environments, navigable waterways, visible night lights, pasture, crops, and population density (Fig. 1). We used pre-existing spatial layers of each pressure, most of which were specific to New Zealand. Some pressure sources were expected to have an effect beyond the source itself. As per the global methodology, we applied a distance-decay relationship for these layers (roads, railways, and navigable waterways). We used the global approach to weight the individual layers before combining them to create an overall metric, which

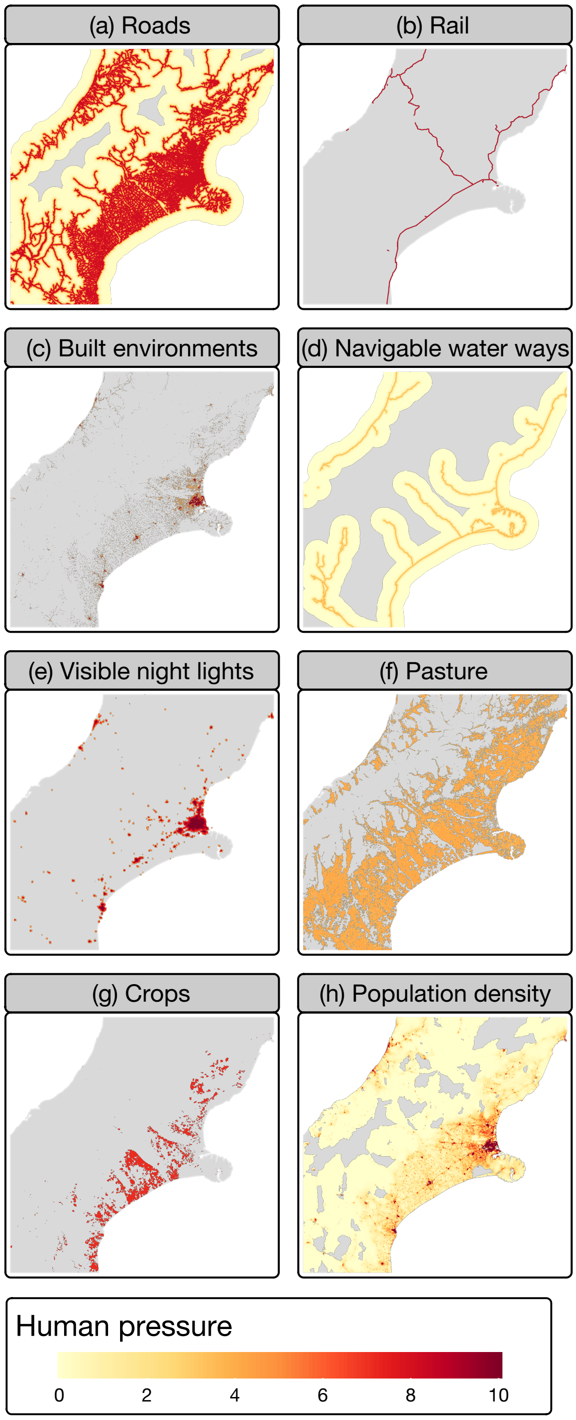

Figure 1. Visualisation of the individual components that make up the combined pressure index, subset to within the Canterbury region for clarity.

ranged from 0 (lowest pressure) to 50 (maximum pressure). Applying the global approach allows for comparability with other national-scale applications of the layer. The New Zealand layer was constrained to the New Zealand coastline (LINZ 2023a).

We generally followed the approach of Sanderson et al. (2002) and Venter et al. (2016a, b) to weight pressure scores, and followed the adaptations of Mu et al. (2022) in relation to night lights. We were able to include dynamic estimates of pasture cover, unlike in previous global estimates of pressure, because we operated at the national scale. We derived a human pressure layer for 2018, as this was the most recent time period in which all data layers were available. We also derived a layer for 2012, an earlier time period for which all data layers were also available. We then quantified how much change had occurred in the 2012–2018 period. We present an overview of our sources and methods in this section, and direct the reader to the Data and Code Availability section for full details relating to data and code used. The Snakemake workflow management system (Mölder et al. 2021) was used to create a reproducible and scalable data analysis, and the major tools used were python 3.11, GDAL 3.7, and QGIS 3.32.

Built environment

We used data produced by the Global Human Settlement Layer, specifically the GHS-BUILT-S R2023A (Pesaresi & Politis 2023). This is a geospatial representation of the built-up surface, expressed in number of square metres per pixel, including both residential and non-residential surfaces, derived from satellite imagery (Sentinel-2 and Landsat). The 2018 year was published at 10 m resolution, but was adjusted to match our resolution of 100 m using a weighted summation.

This was readily converted into a pressure score (F) using equation 1:

$$F = \begin{cases} 10 & \text{if } x > 2000 \\ 4 & \text{if } 0 < x \leq 2000 \\ 0 & \text{otherwise} \end{cases} \tag{1}$$

Note that a fully built-up pixel would have a value of 10 000 (the number of square metres in a 100 m × 100 m pixel), so that, for example, 2000 represents a pixel of which 20% is built up.

Population density

We used the global population density data provided by WorldPop, which produces more precise population estimates than other sources by redistributing aggregated census counts using data, such as building envelopes (Lloyd et al. 2017). WorldPop uses a 1 km² grid, and is focused on low- and middle-income countries where official sources of population density data do not typically exist.

We could have used Statistics New Zealand's geographic data, but this would have caused complications. The statistical standard for geographic areas was recently changed, removing the smallest geographic unit in the statistical geographic hierarchy, the meshblock, when publishing census information (Stats NZ 2023). Instead, two new levels (statistical areas 1 and 2) were introduced, which are composed of contiguous clusters of one or more meshblocks. Meshblocks themselves are not ideal units with which to compute population density, because they include both inhabited and uninhabited (or even uninhabitable) locations, particularly at the margins of settlements. The unavailability of meshblocks for most recent population data compounds this problem. Statistics New Zealand has a prototype population grid (available at 1 km, 500 m, and 250 m resolution) which normalises the geographic unit and would be ideal to use, but this is only published with data from the 2018 census. WorldPop data was therefore used for consistency, and also because it is available with annual population density estimates for the globe, including New Zealand. WorldPop data does appear to have spurious population estimates in unexpected places, including territorial waters. A coastline mask was applied to remove this data, but others spurious estimates may remain; for example, within national parks.

WorldPop data is given in units of people per pixel. Pixels are at 100 m resolution, but the data does not actually use an equal-area projection, so a projection conversion was first made using a weighted sum algorithm to the New Zealand Continental Shelf Lambert Conformal 2000 projection (EPSG:3851). The value (people per 100 m × 100 m pixel) is converted to a pressure score (F) using equation 2:

$$F = \begin{cases} 10 & \text{if } x \geq 10 \\ 3.333 \cdot \log_{10}(x+1) & \text{if } 0 < x < 10 \\ 0 & \text{otherwise} \end{cases} \tag{2}$$

Night-time lights

Annual composite night-time light data were obtained from the Earth Observation Group at the Colorado School of Mines, Annual Visible Infrared Imaging Radiometer Suite (VIIRS) Nighttime lights V2 (Elvidge et al. 2021). Annual composition includes the removal of temporal lights (e.g. fires) and background values, and is ultimately derived from night-time data from the VIIRS Day/Night Band (Cao et al. 2013).

The units are median monthly radiance in units of nW cm^{-2} sr^{-1}. The data was clipped to the same New Zealand geographical area as the other component layers, and then scaled to a 0–65 535 range to facilitate the computation of deciles for the human pressure index. The boundaries of 10 equal deciles were calculated for the 2012 data by ignoring values of 0, and the decile (1 to 10) or 0 was directly used as the pressure score. The breaks for each decile were then applied to the 2018 data to make it comparable to 2012.

Croplands

We used the land-cover information from the Land Cover Database (LCDB) version 5.0 to identify croplands in 2012 and 2018 for mainland New Zealand (MWLR 2020a) and the Chatham Islands (MWLR 2020b). The LCDB data is used by the New Zealand government to assess land cover change (e.g. https://www.stats.govt.nz/indicators/indigenous-land-cover/). We included classes 30 (short-rotation cropland) and 33 (orchards, vineyards, or other perennial crops).

The data was downloaded as a vector and rasterised as a binary raster at 20 m resolution (400 m²). It was then upsampled to 100 m resolution (10 000 m²) with a summation algorithm to obtain a 0–100 value for measuring partial pixel cover at this scale (a value of 20 indicates that 20% of the pixel is covered in cropland). These values were then converted to a pressure score (F) using equation 3:

$$F = \begin{cases} 7 & \text{if } x > 20 \\ 4 & \text{if } 0 < x \leq 20 \\ 0 & \text{otherwise} \end{cases} \tag{3}$$

Pasture

Pasture data was obtained similarly to croplands data. Classes 2 (urban parkland/open space), 40 (high producing exotic grassland), 41 (low producing grassland), and 44 (depleted grassland) were all included in this definition.

The cover values were obtained in the same fashion as for cropland and were converted to a pressure score (*F*) using equation 4:

$$F = \frac{x}{100} \cdot 4 \tag{4}$$

Roads

We obtained 1:50 000 scale road centreline data from Land Information New Zealand's topographic data (LINZ 2023b, c). All data in this series have a stated planimetric accuracy of ± 22 m, although it is not recorded whether a road is public or private. Tunnels were erased from the set of roads with a 1 m tolerance using a process that does not affect surface roads situated above tunnels. Roads were rasterised to the same grid with a 100 m resolution (10 000 m^2) using the Geospatial Data Abstraction Library (not using the "all touched" rasterisation strategy).

We measured Euclidean distance (m) from roads. This proximity information was then converted to a pressure score (*F*) using equation 5:

$$F = \begin{cases} 8 & \text{if } x \le 500 \\ 3.75 \cdot \exp\left(-1 \cdot \left(\frac{x}{1000} - 1\right)\right) + 0.25 & \text{if } 500 < x < 15000 \\ 0 & \text{otherwise} \end{cases} \tag{5}$$

A temporal component of roads (and tunnels) was captured through the novel use of Kart (Kart contributors 2023), a distributed version-control software for geospatial data. This software allowed us to represent the topographic roads data at specific points in time (from 2012 to the present) in order to capture the state of the road network as it developed over time (e.g. excluding the most recently completed highways when analysing earlier time periods).

Railways

Railway centrelines were obtained using the same method used for roads (LINZ 2023d), including accounting for tunnels and using Kart to represent temporality (although this is less relevant for railways). Straight-line distance from railway lines was calculated and converted to a pressure score (*F*) using equation 6:

$$F = \begin{cases} 8 & \text{if } x \le 500 \\ 0 & \text{otherwise} \end{cases} \tag{6}$$

Navigable waterways

For the purposes of human pressure mapping, navigable waterways were defined as waterways where the depth is greater than 2 m, as well as all coastlines and major lakes. Major lakes were derived from those lakes present in Land Information New Zealand's 1:500 000 scale topographic mapping (LINZ 2023e). The exterior ring of the lake was obtained (the lake was represented as a line rather than a polygon) and then rasterised. The coastline was taken as the mean high water at 1:50 000 scale (LINZ 2023a), and was rasterised.

Rivers were obtained from River Environment Classification (REC2) New Zealand (Snelder & Biggs 2002), but this database does not have depth information. Depth was estimated on the basis of estimated discharge rates for REC2 rivers, available at New Zealand River Maps (Whitehead & Booker 2020). Estimated discharge rates were converted to depth estimates using the following equations (7–9) from Williams et al. (2020), which assume that the shape of a river channel can be described using a second-order parabola:

$$\text{velocity} = 4 \cdot \frac{\text{discharge}[\text{m}^3\text{s}^{-1}]^{0.6}}{\text{width}[\text{m}]} \tag{7}$$

$$\text{cross-sectional area} = \frac{\text{discharge}}{\text{velocity}} \tag{8}$$

$$\text{depth}[\text{m}] = 1.5 \cdot \frac{\text{cross-sectional area}}{\text{width}} \tag{9}$$

Certain parameters were already given by New Zealand River Maps data:

(1) discharge: median flow (cumecs)—the predicted median of mean daily flow time-series over all time;

(2) width: width at median flow (m)—wetted width across the river channel at median flow.

Rivers were filtered so that only reaches with depths greater than 2 m were retained as navigable waterways. Rivers were represented in REC2 as flowing through lakes; these parts were erased in the raster representation of rivers using the lakes dataset, such that when the rasterised representations of rivers, lakes and coastlines were combined, there was a raster representation of only the edges of lakes, as well as all coastlines and navigable rivers.

Using VIIRS night-time lights data (previously described), any navigable water within 4 km (Euclidean) of a lit pixel (of any brightness) was identified as a source area in our subsequent calculations. In these calculations, we identified any navigable waterway pixel within 80 km of a source pixel along the network of navigable waterways using the GRASS GIS "r.cost" function, progressing from source pixels. Traversal beyond navigable waterways (i.e. over land, or across a lake or inland sea) was not considered possible in this model. Once identified, areas near navigable waterways were converted to a pressure score using equation 10:

$$F = \begin{cases} 0 & \text{if } x \ge 15000 \\ 4 \cdot \exp(-1 \cdot x) & \text{otherwise} \end{cases} \tag{10}$$

Compiling the New Zealand human pressure index

All eight components (Fig. 1) were combined additively.

The New Zealand coastline (1:50 000 scale) was reused in this final step in order to firmly set no-data values for marine spaces. Outside marine areas, the minimum value was 0. This resulted in a raster layer where all terrestrial spaces had values ranging from a minimum of 0 to a hypothetical maximum of 50. Following Williams et al. (2020), built environments, cropland, and pasture followed a "land-use exclusion principle" whereby the three types may not co-occur. Although the individual pressure values were calculated independently, at the combination stage the first non-zero value among built, cropland, and pasture pressure components was taken, in that order. If this were not the case, and summation were performed naïvely, the hypothetical maximum value would be 61.

The output datatype was 32-bit floating-point (i.e. not rounded), rather than an integer, because some components used logarithmic or exponential functions and the values were not rounded.

Difference between global and local datasets

To compare the global and local datasets, we created a raster layer of the differences between each cell for the local and global versions. We accomplished this by aggregating the New Zealand layer to the coarser resolution (i.e. from 100 × 100 m to 1 × 1 km cells) and then subtracting the value of each cell in the New Zealand layer from that of the corresponding cell in the global layer. We present the summary statistics, based on a random sample of 10 000 non-null values (extracted using the "spatSample" function from the terra package; Hijmans 2023), along with a map of the differences (Fig. 2).

Differences between local datasets over time

We sampled 10 000 non-null raster cells from the 2012 layer using the "spatSample" function from the terra package (Hijmans 2023), but this time extracted the spatial locations and used these locations to sample 10 000 cells from the same locations in the 2018 layer (also all non-null). We then used bootstrapping (Davison & Hinkley 1997) to calculate the mean and 95% confidence interval for differences over time. We present the 2018 human pressure layer for New Zealand (Fig. 3), and the extreme values of the distribution of differences between each raster cell (Appendix S1 in Supplementary material).

Amount of wilderness, intact, and highly modified land

For 2018 we classified values as per the global synthesis of Mu et al. (2022), where <1 is "wilderness", 1 to <4 is "intact", and ≥4 is "highly modified". We calculated the frequency of each category in the resulting classified raster and expressed the result as the percentage of New Zealand that falls into each category. We used the number of non-null cells as the denominator in the equation.

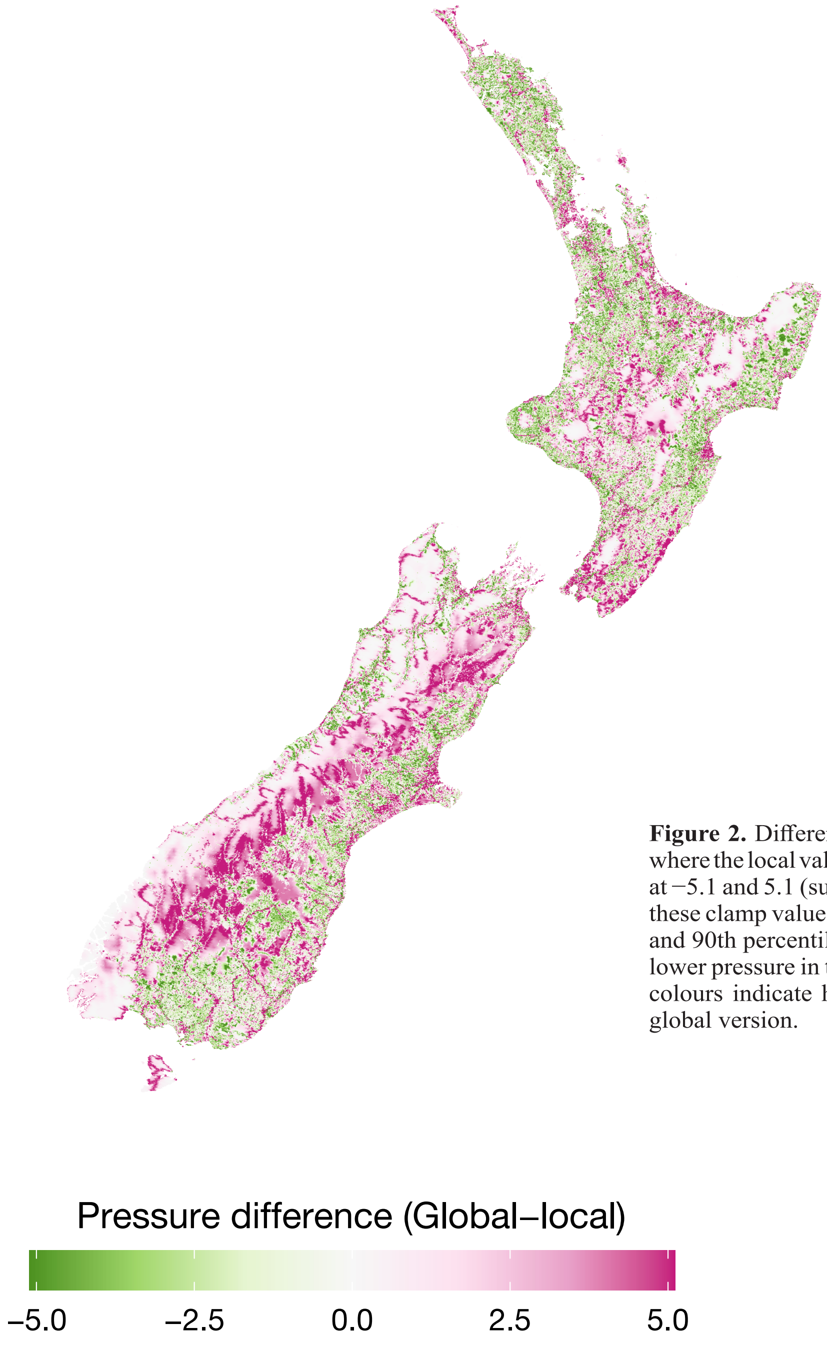

Figure 2. Difference between global and local human pressure layers, where the local value is subtracted from the global. The values are clamped at −5.1 and 5.1 (such that values beyond these are shown as these limits); these clamp values were taken from the largest absolute value of the 10th and 90th percentile of the difference (see results). Pink colours indicate lower pressure in the local version compared to the global version, green colours indicate higher pressure in the local version compared to the global version.

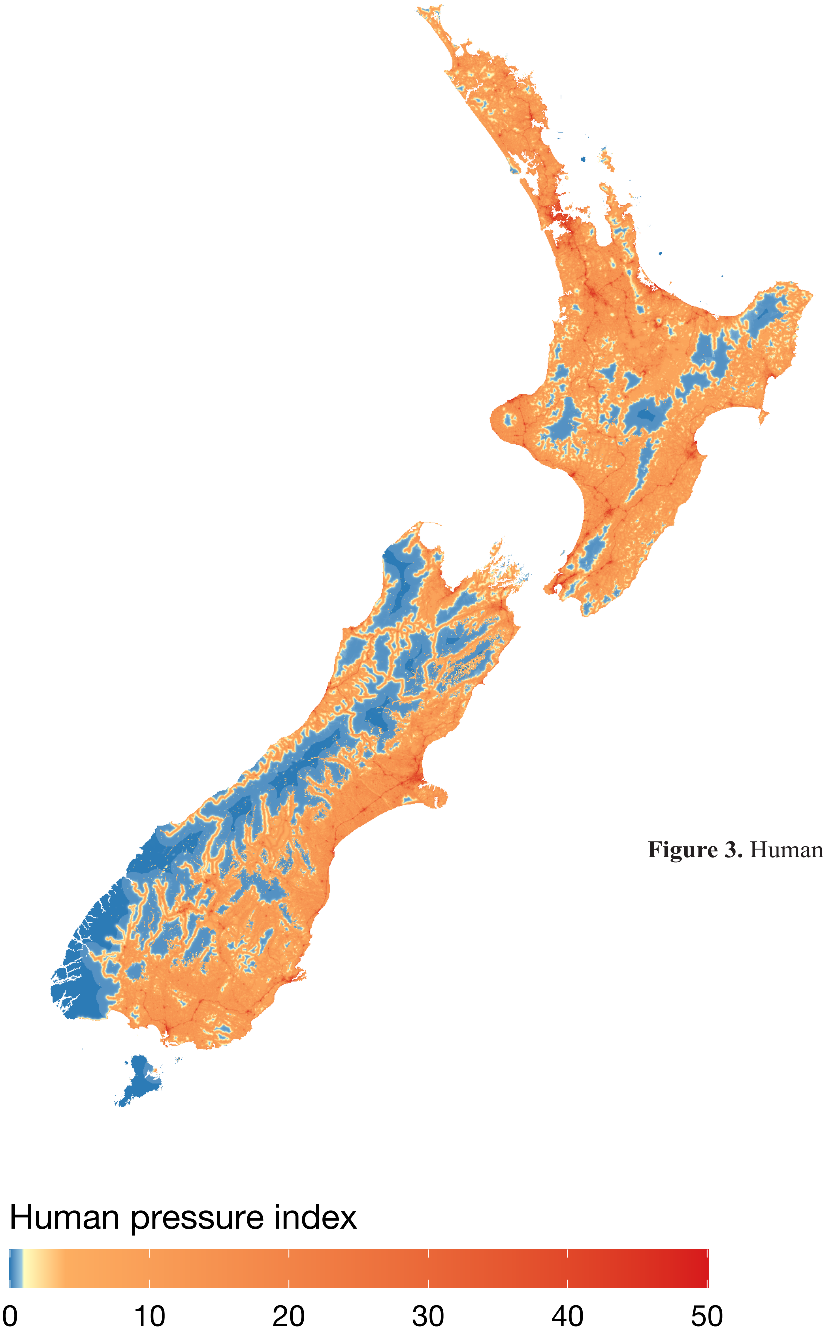

Figure 3. Human pressure map for New Zealand for 2018.

Example use case one: differences between IUCN categories of land

In this case study, we assessed whether categories of New Zealand's protected conservation land, as ranked by the IUCN protection criteria (Bellingham et al. 2016), correlate with the 2018 human pressure scores for that land.

We extracted the pressures for categories of national conservation land (Table 1) that correspond to the IUCN categories of protection 1A through 5, where 1A is a "strict nature preserve", and is the most protected category of land, and 5 is "protected landscape/seascape", which is the least protected category. These categories of conservation land represent a subset of the land held for conservation purposes, but we considered them to provide illustrative examples.

We included all areas that had a human pressure score available, and present summary statistics visualised as a boxplot, where the lower hinge is the 25th percentile, the middle of the box is the median, the upper hinge is the 75th percentile, and the whiskers represent each extreme within the data that is within 1.5 times the interquartile range (Fig. 4). Data beyond the whiskers were considered 'outliers' and were plotted individually. We included all pixels without summarising across polygons first in order to give equal weight to each included pixel, irrespective of the size of the polygon.

We then extracted the individual pressure scores to assess any differences that arose. Scenic Reserves (IUCN category 3) were the primary outlier in the overall analysis, with a higher pressure than was exhibited in the lower ranked categories

Table 1. Description of data used in analysis: New Zealand protected land categories by IUCN protection ranking (as per Bellingham et al. (2016)), and New Zealand protection status.

IUCN category	NZ category	Act	Section
1A	National Parks (Specially Protected Areas)	National Parks Act 1980	s12
1B	National Parks (Wilderness Areas)	National Parks Act 1980	s14
2	Conservation Parks	Conservation Act 1987	s19
3	Scenic Reserves	Reserves Act 1977	s19(1)(a)
4	Stewardship Areas	Conservation Act 1987	s25
5	Recreation Reserves	Reserves Act 1977	s17

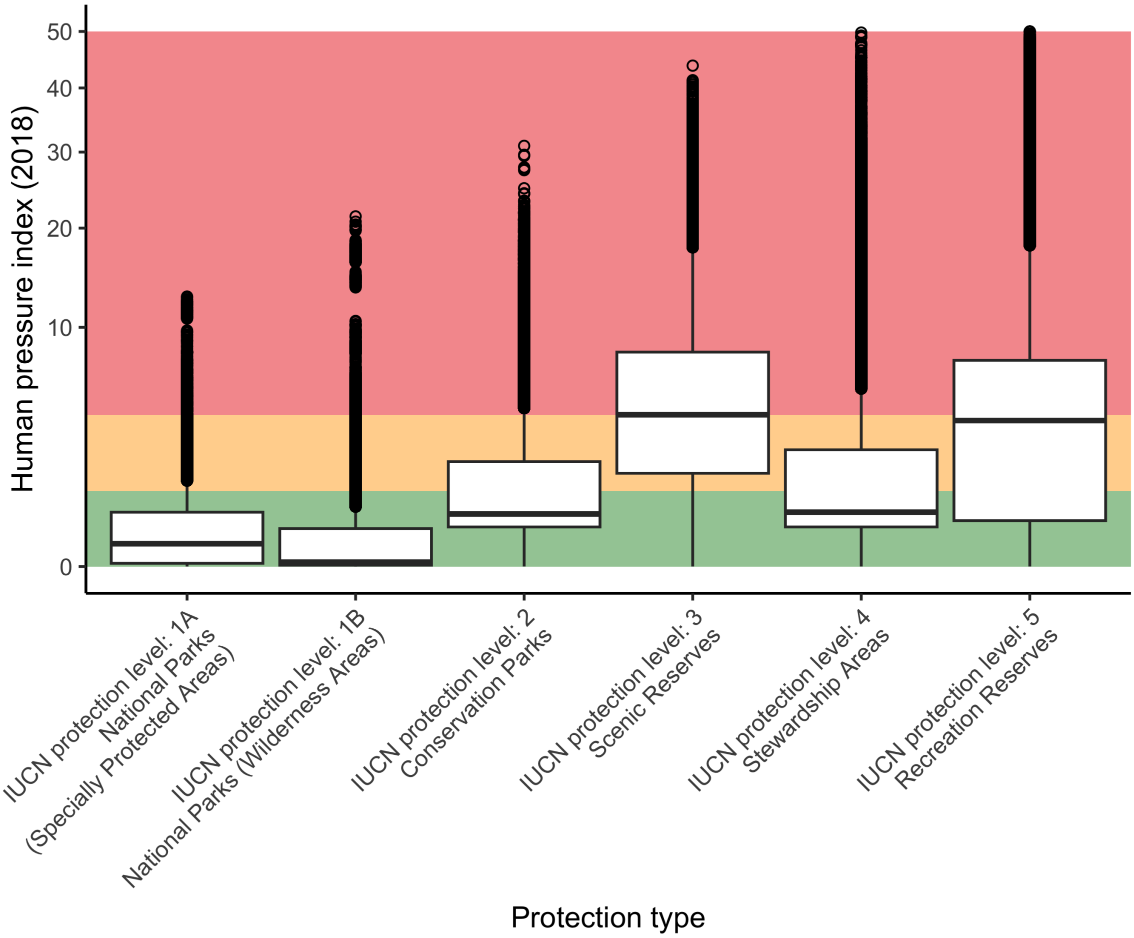

Figure 4. Human pressure levels within different types of conservation parks in New Zealand. The green shading indicates pressure scores that correlate to "wilderness", orange shading to "intact", and red to "highly modified". Square-root scale used on y-axis.

IUCN 4 and IUCN 5 (Stewardship Areas and Recreation Reserves), so we assessed pressures by type for each. We present these as a boxplot, which represents the same statistics as described above (Fig. 5).

Example use case two: linking wetland loss to increasing pressure

In a second use case, we used the 2012 human pressures data to assess whether pressures in 2012 predicted the loss of wetlands between 2012 and 2018 compared to wetlands that were maintained over the same time period. We used LCDB wetland coverage data for mainland New Zealand (MWLR 2020a), selecting wetland polygons that existed in 2012, and then noted whether they continued to exist in 2018. We extracted the 2012 pressures (overall, and the individual components) for all polygons. We assessed whether the lost wetlands had a higher human pressure using summary statistics and a density plot. We then used summary statistics to examine the individual pressure components to assess why any differences arose.

Results

In general and as expected from our methodology, we found human impact to be concentrated around major urban settlements and along transport corridors (Fig. 3). The South

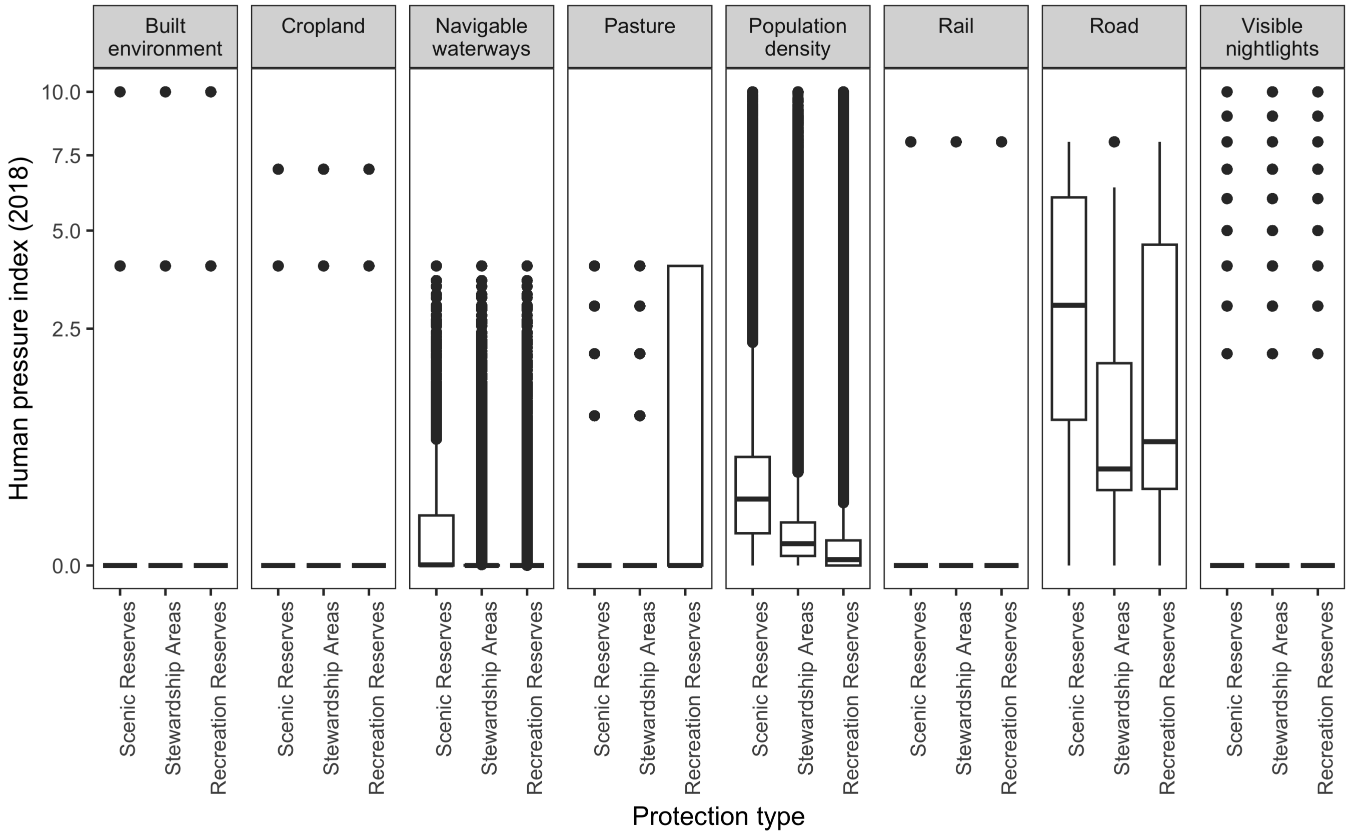

Figure 5. Human pressures by component types, for Scenic Reserves (IUCN category 3), Stewardship Areas (IUCN category 4), and Recreation Reserves (IUCN category 5). Note that not all pressures can reach the y scale maximum (10); however, we draw attention to the pressure components for which Scenic Reserves score relatively highly, thus driving their outlier status with higher-than-expected pressure. Square-root scale used on y-axis.

Island of New Zealand (and off-shore islands such as Stewart Island) had notably larger areas of low pressure land compared to the North Island (Fig. 3).

Global to local spatial differences

Overall, the median sampled difference between the local and global layers for 2018 was 0.65, while the 10th and 90th percentiles of the difference were −3.46 and 5.14, respectively. We assessed the difference visually (see Fig. 2) and found that higher local pressure appeared to relate to differences in our treatment of night-time lights. This likely arises because the global dataset also uses deciles, but the deciles take into account the entire globe, whereas the deciles for the local layer only account for relative differences within New Zealand. Conversely, we found reduced local pressure around river valleys, particularly in the South Island, and around parts of southern Stewart Island. We speculate that this relates to a more inclusive “pasture” definition under the global layer, or to some differences in the data underlying navigable water ways; however, unlike the national data we present, the global layer (Mu et al. 2022) did not release individual component pressures with their combined layer.

Temporal differences

For temporal differences between the local layers, there was a near-zero change of 0.093 between the 2012 and 2018 local layers, where the 95% confidence interval was 0.072–0.113. The spatial distribution of areas of larger change is shown in Appendix S1.

Amount of wilderness, intact, and highly modified land

The majority of New Zealand (60%) qualifies as “highly modified”; see Table 2. The category with the next highest proportion of coverage is “wilderness” (very low pressure), at 28%, followed by “intact” (low pressure) land (12%).

Example use case one: differences between IUCN categories of land

The highest levels of IUCN protection categories (1A and 1B) were reflected by a very low pressure distribution (Fig. 4). The IUCN levels 2 and 4 (Conservation Parks and Stewardship Areas, respectively) also had medians placing them in the “wilderness” or very low pressure range. The highest levels of modification occurred within IUCN level 3 (Scenic Reserves) and IUCN level 5 (Recreation Reserves) (Fig. 4).

As a result of these findings, we assessed each pressure component for IUCN levels 3 (Scenic Reserves), 4 (Stewardship Areas), and 5 (Recreation Reserves) (Fig. 5). Pasture (i.e. grassland) featured as a component in some Recreation Reserves under our model, although the median pressure value was 0 for all three IUCN levels. There were two categories in which Scenic Reserves had the highest median pressure. Road pressures contributed a median value of 2.9 to Scenic Reserves, compared to 0.41 for Stewardship Areas and 0.68

for Recreation Reserves. Population density had the highest median for Scenic Reserves (0.20) compared to Stewardship Areas (0.02) and Recreation Reserves (0.00).

Example use case two: linking wetland loss to increased pressure

We assessed whether wetlands mapped at the national scale in 2012 that were lost by 2018 had a different pressure environment (represented by a 100 m buffer around each polygon) than wetlands that remained. Overall, the median pressure value for wetlands that were lost and those that were maintained was similar (9.8 for both). The difference lay at the lower end of the distribution, where minimum pressures around wetlands that were lost were higher than for those that were maintained (the 25th percentile was 7.1 for wetlands that were lost, compared to 4.3 for wetlands that were maintained; Fig. 6a).

Table 2. Percentage of wilderness, intact, and highly modified land in New Zealand as of 2018. Following convention, square brackets indicate that a number is included within a range; curved brackets indicate a number is excluded.

Description	Pressure	Percent NZ
Wilderness	[0–1)	28%
Intact	[1–4)	12%
Highly modified	[4–50]	60%

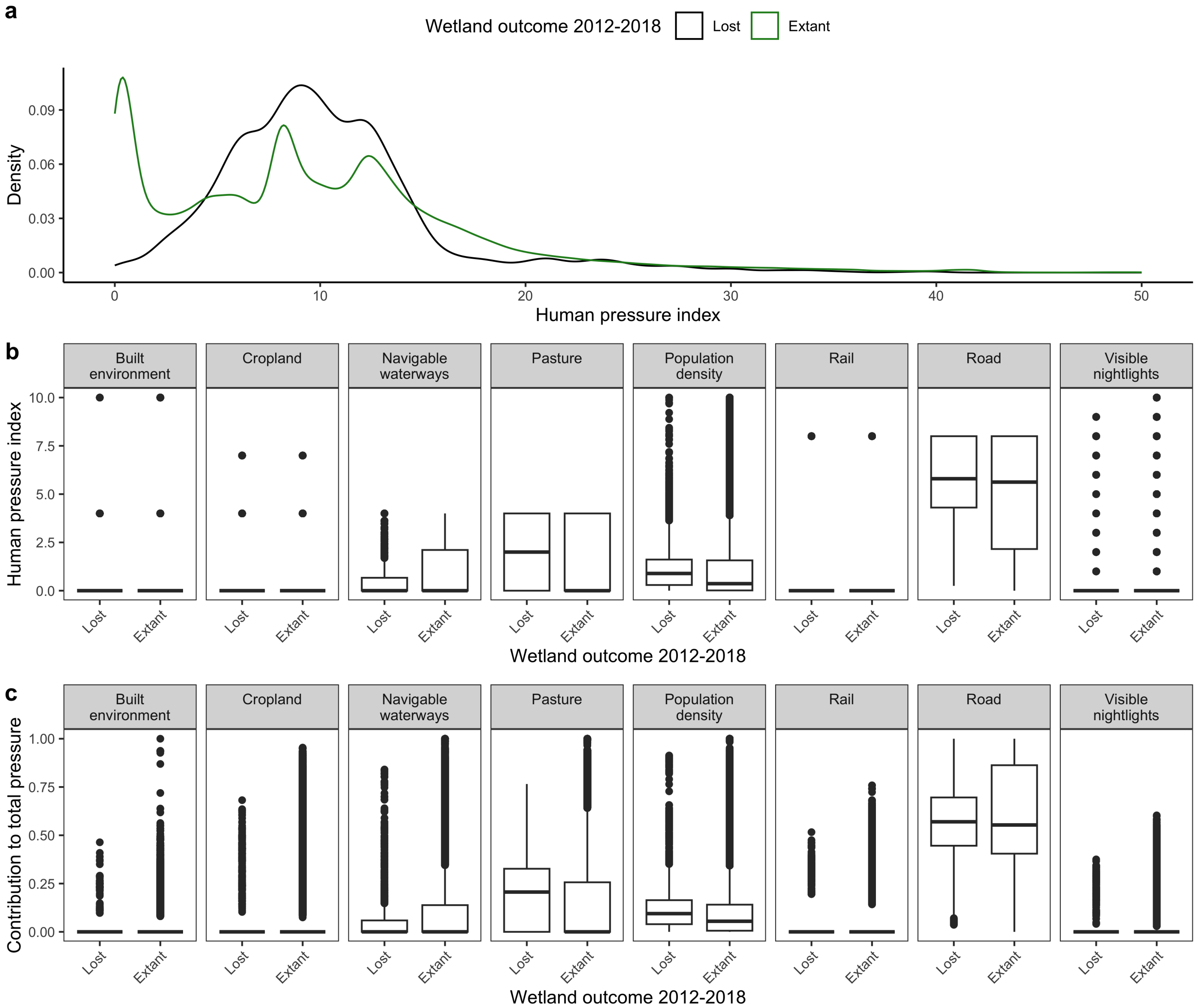

Figure 6. (a) Difference in pressure distributions for wetlands that remained extant during the period 2012–2018 (note the largest peak at very low pressures, and then a second, wider peak at more moderate pressures), and wetlands that were lost during the period 2012–2018 (note a single broad peak centred around a pressure value of c. 10). (b) Differences in component pressures for extant wetlands and wetlands lost for the period 2012–2018. Individual outliers are shown but appear near-categorical for the human pressure index in some panels because of the limited number of outcomes possible (e.g. rail can have a pressure value of 8 or 0 only). (c) Differences in the relative contribution of component pressures for extant wetlands and wetlands lost, for the period 2012–2018.

We examined the individual pressure components for lost and remaining wetlands and found that roads, pasture, and population density were higher in the areas around lost wetlands compared to those that remained (Fig. 6b), and also formed a relatively higher proportion of the total pressures around each wetland (Fig. 6c).

Discussion

Human pressure layers are important for mapping threats to biodiversity and prioritising conservation efforts, but global layers can miss important local context, and are often at a coarse scale that renders them inapplicable to national-scale analysis. Here we create a New Zealand human pressure index based on the methodology of the global Human Footprint Map, to allow comparison with other countries, but taking advantage of national-scale data where available. We assembled a human pressure layer that included eight components: built environments, cropland, navigable waterways, pasture, population density, rail, roads, and visible night lights.

We created a localised version of the global Human Footprint Map which used a more suitable projection, and was at a scale more suitable to national or regional analyses (0.01 km^2 for the national layer cf. 1 km^2 for the global layer). We found this layer, and the underlying individual pressure component layers, to be useful for understanding (a) pressures on protected land across different levels of internationally comparable protection, and why Scenic Reserves had a disproportionately high level of pressure within them, and (b) how pressures around wetlands, particularly pressures relating to pasture and roads, differentiate wetlands that were lost between 2012 and 2018 from those that remained extant in that period.

The local layer revealed that 28% of New Zealand's terrestrial area can be classified as "wilderness" while 60% is "highly modified". This is consistent with the global wildnerness estimate of 28% in 2018, although these global results varied by biome and the number was driven upwards by high proportions of wilderness in tundra and boreal forests/taiga, neither of which are found in New Zealand (as per Mu et al. 2022, who used the Olson et al. 2001 biome classification). In contrast, globally for temperate broadleaf and mixed forests (dominant wilderness ecotypes for New Zealand), the remaining wilderness was estimated at only 5%; for montane grasslands and shrublands it was 19%, and for temperate grasslands, savannahs, and shrublands, it was 1.74%. These values indicate that in comparison to other areas around the globe falling in the same major biomes as New Zealand, New Zealand has relatively more wilderness remaining.

We found no real difference in the total human pressure for New Zealand for the 2012 and 2018 time periods we considered. The mean difference was 0.093 (95% confidence interval: 0.072–0.113). This can be compared to a global increase of 9% in the time period 1993–2009 globally, although the highest income countries had a small decrease in the same period (Venter et al. 2016a). The numbers are clearly not directly comparable, because of the different time periods considered. Venter et al. (2016a) examined some of the correlates of pressure change, such as changes in population and gross domestic product, and we consider that this would be a worthwhile direction for future work.

Internationally, protected land can vary from "paper parks", protected only on paper (Bruner et al. 2001), to strict protection with armed guards (Duffy 2014; Vimal et al. 2021; Day et al. 2023). The human pressure index in Indonesia showed increases in pressure within and around national parks driven by human density and accessibility (Dwiyahreni et al. 2021). We found that pressures within different reserves in New Zealand increased in correlation with their IUCN protection status, except for Scenic Reserves. An analysis of the different pressure contributions found that roads and population density had a higher impact in Scenic Reserves than in less protected areas. This does not mean that there are roads are within Scenic Reserves, nor that people live within them. As noted in the Methods, the size of the pixels for population density means that some leakage occurs. With regards to roads, we used a distance decay function, which means that roads near Scenic Reserves apply pressures to them (Viles & Rosier 2001; contrast Sullivan et al. 2009). In fact, the preponderance of roads near Scenic Reserves (or Scenic Reserves near roads) was noted by Molloy (2015). Overall, as IUCN categories relate to protection rather than risk, we do not consider our findings inconsistent with the rankings of Bellingham et al. (2016).

In our second example use case we examined whether pressures around, rather than within, wetlands were associated with subsequent wetland loss in New Zealand. During the period 2012–2018, 1681 ha of wetlands were lost, of those that are mapped at the national scale. This was a test of whether the human pressure layer might usefully be used as a metric to predict increasing risks to ecosystems, as it has been used internationally to predict changes in species extinction risks (Di Marco et al. 2018) and to improve conservation decision-making (Tulloch et al. 2015).

We found that the distribution of pressures around wetlands in 2012 that were lost in the period 2012–2018 was quite different to the distribution of pressures around wetlands that were maintained over the same period. Pressures around wetlands that were lost had a unimodal distribution centred around a pressure score of c. 10. Wetlands that were retained had (broadly speaking) a bi-modal distribution, with the largest peak representing very low pressures around wetlands, and a second, broader peak more closely mirroring that of the pressures around wetlands that were lost. We suggest that a rate-of-change analysis of human pressures undertaken with annual timesteps would provide a more nuanced perspective; that was not possible with the data we were able to produce.

Recent work has indicated that most freshwater wetland loss (90%; Ausseil et al. 2011) in New Zealand is associated with conversion to high-producing grassland, usually co-occurring with dairy farming (Robertson et al. 2019; Denyer & Peters 2020). This was reflected by our analysis of the relative contribution of individual pressures that make up the index: while the biggest overall pressure was distance from roads, this applied to wetlands both lost and extant. The biggest difference in median pressures that affected lost wetlands compared to extant wetlands was the area of pasture within 100 m of the wetland (median value of 2 for lost wetlands, and 0 for extant wetlands; median proportion pressure contribution of 0.206 for lost wetlands, and 0 for extant wetlands).

Although LCDB data were used in calculating the pressure index and (separate) LCDB data were used to assess wetland extent, we do not consider our results to be circular for two reasons. Firstly, wetland cover is technically uncorrelated with the landcover in the LCDB, as it is a separate attribute. A polygon of low-producing grassland (one of our LCDB categories that made up pasture) could simultaneously be detected as wetland, if wet enough. Secondly, even to the extent that wetland cover and land cover are correlated in practice, we assessed the pressures in a 100 m buffer around wetlands and excluded the area within the wetland itself.

Limitations

Our layer is based on national-scale mapping, such as the LCDB, and can be considered no more accurate than the underlying data. Highly local analyses (where one would not consider the LCDB's minimum polygon size of 1 ha to be appropriate, for example) should instead seek out finer-scale data layers and recalculate a pressure index.

The concept of a human pressure index is, by necessity, a simplification. We acknowledge that there will be species that may find an increase in habitat, or at least a relatively lower decline in loss of habitat, compared to other species, with an increase in pressure. For example, we consider high-producing grassland as representing ecological pressure (and we would contend that overall, it is), but it does hold habitat value for kererū who forage on clover (Burge et al. 2021). Overall, we consider habitat provision does not negate the pressure that some land covers represent on the environment as a whole, but acknowledge the same land cover will have different outcomes for different species.

Future work and improvements

We produced a terrestrial pressure layer, which means that the area outside the coastline is ignored (i.e. near-coast ocean such as intertidal harbours). This is unfortunate for a country with so much coastline and acknowledged pressures on it. We note the recent work on a global coastal layer by Allan et al. (2023) and we hope that our methodology might be adapted, in conjunction with the methodology of Allan et al., to provide a national-scale coastal layer in the future.

Future work (aside from a potential coastal layer) might usefully include a longer time series of pressures, like the annualised pressure layers in Mu et al. (2022). The two factors that currently constrain this are the inter-annual timesteps of the LCDB, which is used in several of the pressure components, and the scale of the human population data, which is currently drawn from global data, and is at the 1 km^2 scale. This coarse scale is a limitation of our paper. While the WorldPop global data sources have been independently validated (Lloyd et al. 2017), a local validation has not occurred in New Zealand. A visual analysis did reveal that WorldPop data does appear to have spurious population estimates in unexpected places, including in territorial waters, and this was resolved by limiting the data to the New Zealand coastline. If the currently-trialled population grids by Statistics New Zealand are provided for time steps beyond the current one, this would allow much finer-grained population analysis than the currently available mesh block data allows, and would represent an improvement over global data.

Finally, a more highly localised version of this layer could be considered for development by those who seek a spatial layer of New Zealand-specific pressures (e.g. following those listed in Dymond & Ausseil 2019); this is supported by Woolmer et al. (2008). An additional consideration might be the inclusion of plantation forestry in the cropland pressure layer. Inclusion of plantation forestry has precedent in other regionalised human pressure calculations, such as that by Dwiyahreni et al. (2021) who calculated human pressure change in and around Indonesia's national parks. It would also be ecologically justified in New Zealand given the invasion pressures that plantations potentially represent (Davis et al. 2011; Bellingham et al. 2023) and the periodic large-scale disturbance caused by removal of vegetation cover during harvesting. A localised version might also allow for a more subtle differentiation of the intensity of the pressure from different parts of the road network (e.g. differentiating highways from unsealed, low usage roads) as adopted by Dwiyahreni et al. (2021). It could also differentiate between different LCDB categories of intensity within pasture, such as "High Producing Grassland" and "Low Producing Grassland". Such a localised version would limit the comparability with international work, however.

Acknowledgements

We acknowledge input from other members of New Zealand's Biological Heritage National Science Challenge think tank, Aroha Mead and Jason Tylianakis. We thank three anonymous reviewers, and James McCarthy (Manaaki Whenua – Landcare Research), for comments on earlier versions of this manuscript.

Additional information and declarations

Data and code availability: data and a link to the code are available via Datastore (https://doi.org/10.7931/7pm3-xp10).

Funding: we acknowledge funding by New Zealand's Biological Heritage National Science Challenge and Strategic Science Investment Fund for Crown Research Institutes from the New Zealand Ministry of Business, Innovation and Employment's Science and Innovation Group.

Conflicts of interest: the authors have no conflicts of interest to declare.

Ethics: no permits or approvals were required to undertake this work.

Author contributions: Olivia Burge: conceptualisation, methodology, investigation, writing – original draft, visualization, supervision, project administration. Richard Law: methodology, visualisation, software, data curation, writing – review and editing. Sandy Wakefield: conceptualisation, writing – review and editing.

References

Allan H, Levin N, Kark S 2023. Quantifying and mapping the human footprint across earth's coastal areas. Ocean & Coastal Management 236: 106476.

Ausseil A-GE, Chadderton WL, Gerbeaux P, Stephens RTT, Leathwick JR 2011. Applying systematic conservation planning principles to palustrine and inland saline wetlands of New Zealand. Freshwater Biology 56(1): 142–161.

Bellingham PJ, Overton JMcC, Thomson FJ, MacLeod CJ, Holdaway RJ, Wiser SK, Brown M, Gormley AM, Collins D, Latham DM, Bishop C, Rutledge DT, Innes JG, Warburton B 2016. Standardised terrestrial biodiversity indicators for use by regional councils. Lincoln, Landcare Research. 426 p.

Bellingham PJ, Arnst EA, Clarkson BD, Etherington TR,

Forester LJ, Shaw WB, Sprague R, Wiser SK, Peltzer DA 2023. The right tree in the right place? A major economic tree species poses major ecological threats. Biological Invasions 25(1): 39–60.
Bruner AG, Gullison RE, Rice RE, da Fonseca GAB 2001. Effectiveness of parks in protecting tropical biodiversity. Science 291(5501): 125–128.
Burge OR, Innes JG, Fitzgerald N, Guo J, Etherington TR, Richardson SJ 2021. Assessing the habitat and functional connectivity around fenced ecosanctuaries in New Zealand. Biological Conservation 253: 108896.
Burge OR, Price R, Wilmshurst JM, Blyth JM, Robertson HA 2023. LiDAR reveals drains risks to wetlands have been under-estimated. New Zealand Journal of Ecology 47(1): 3523.
Cao C, Xiong J, Blonski S, Liu Q, Uprety S, Shao X, Bai Y, Weng F 2013. Suomi NPP VIIRS sensor data record verification, validation, and long-term performance monitoring. Journal of Geophysical Research: Atmospheres 118(20): 11664–11678.
Clarkson BR, Ausseil A-GE, Gerbeaux P 2013. Wetland ecosystem services. In: Dymond JR ed. Ecosystem services in New Zealand. Lincoln, Manaaki Whenua Press. Pp. 192–202.
Davis M, Coker G, Howell C, Henley D 2011. Establishment of *Pseudotsuga menziesii* and *Pinus nigra* seedlings in *Kunzea ericoides* and *Leptospermum scoparium* shrubland communities. New Zealand Journal of Ecology 35(3): 280–286.
Davison AC, Hinkley DV 1997. Bootstrap methods and their applications. Cambridge, Cambridge University Press. 582 p.
Day C, Moreto W, Ravary R 2023. Ranger/soldier: patterns of militarizing conservation in Uganda. Journal of Eastern African Studies 17(1–2): 57–78.
Denyer K, Peters M 2020. The root causes of wetland loss in New Zealand: An analysis of public policies & processes. Wetland Trust, Hamilton. 36 p.
Di Marco M, Venter O, Possingham HP, Watson JEM 2018. Changes in human footprint drive changes in species extinction risk. Nature Communications 9(1): 4621.
Duffy R 2014. Waging a war to save biodiversity: the rise of militarized conservation. International Affairs 90(4): 819–834.
Dwiyahreni AA, Fuad HAH, Muhtar S, Soesilo TEB, Margules C, Supriatna J 2021. Changes in the human footprint in and around Indonesia's terrestrial national parks between 2012 and 2017. Scientific Reports 11(1): 4510.
Dymond J, Ausseil A-G 2019. An ecosystem services approach to choosing environmental indicators for state of environment reports. New Zealand Science Review 75(2–3): 43–51.
Elvidge CD, Zhizhin M, Ghosh T, Hsu F-C, Taneja J 2021. Annual time series of global VIIRS nighttime lights derived from monthly averages: 2012 to 2019. Remote Sensing 13(5): 922.
Hijmans RJ 2023. Terra: Spatial data analysis. V. 1.7-78. https://CRAN.R-project.org/package=terra.
Kart contributors 2023. Kart geospatial data version-control software. V. 0.15.1. https://kartproject.org.
LINZ 2023a. NZ Coastline - mean high water (1:50K). https://data.linz.govt.nz/layer/105085-nz-coastline-mean-high-water/ (accessed 1 July 2024).
LINZ 2023b. NZ road centrelines (topo, 1:50k). https://data.linz.govt.nz/layer/50329-nz-road-centrelines-topo-150k/ (accessed 1 July 2024).
LINZ 2023c. NZ Chatham Island road centrelines (Topo, 1:50k). www.linz.govt.nz/topography/topo-maps/topo50 (accessed 1 July 2024).
LINZ 2023d. NZ railway centrelines (Topo, 1:50k). https://data.linz.govt.nz/layer/50319-nz-railway-centrelines-topo-150k/ (accessed 1 July 2024).
LINZ 2023e. NZ lake polygons (Topo, 1:500k). https://data.linz.govt.nz/layer/50212-nz-lake-polygons-topo-1500k/ (accessed 1 July 2024).
Lloyd CT, Sorichetta A, Tatem AJ 2017. High resolution global gridded data for use in population studies. Scientific Data 4(1): 170001.
McCarthy J, Leathwick J, Roudier P, Barringer J, Etherington T, Morgan F, Odgers N, Price R, Wiser S, Richardson S 2021. New Zealand Environmental Data Stack (NZEnvDS): a standardised collection of spatial layers for environmental modelling and site characterisation. New Zealand Journal of Ecology 45(2): 3440.
Mölder F, Jablonski KP, Letcher B, Hall MB, Tomkins-Tinch CH, Sochat V, Forster J, Lee S, Twardziok SO, Kanitz A, Wilm A, Holtgrewe M, Rahmann S, Nahnsen S, Köster J 2021. Sustainable data analysis with Snakemake. F1000Research 10: 33.
Molloy L 2015. Scenic, historic, recreation and other reserves. Ministry for Culture and Heritage Te Manatu Taonga. https://teara.govt.nz/en/protected-areas/page-4 (accessed 27 November 2023).
Mu H, Li X, Wen Y, Huang J, Du P, Su W, Miao S, Geng M 2022. A global record of annual terrestrial human footprint dataset from 2000 to 2018. Scientific Data 9(1): 176.
MWLR 2020a. Land Cover Database version 5.0, Mainland New Zealand. doi:10.26060/W5B4-WK93.
MWLR 2020b. Land Cover Database version 5.0, Chatham Islands. doi:10.26060/ETRS-VH40.
Olson DM, Dinerstein E, Wikramanayake ED, Burgess ND, Powell GVN, Underwood EC, D'amico JA, Itoua I, Strand HE, Morrison JC, Loucks CJ, Allnutt TF, Ricketts TH, Kura Y, Lamoreux JF, Wettengel WW, Hedao P, Kassem KR 2001. Terrestrial ecoregions of the world: a new map of life on earth: a new global map of terrestrial ecoregions provides an innovative tool for conserving biodiversity. BioScience 51(11): 933–938.
Patterson MG, Cole AO 2013. 'Total economic value' of New Zealand's land-based ecosystems and their services. In: Dymond JR ed. Ecosystem services in New Zealand – conditions and trends. Lincoln, Manaaki Whenua Press. Pp. 496–510.
Pesaresi M, Politis P 2023. GHS-BUILT-S R2023A - GHS built-up surface grid, derived from Sentinel2 composite and Landsat, multitemporal (1975-2030). European Commission, Joint Research Centre (JRC). http://data.europa.eu/89h/9f06f36f-4b11-47ec-abb0-4f8b7b1d72ea (accessed 1 July 2024).
Reid JL, Fagan ME, Zahawi RA 2018. Positive site selection bias in meta-analyses comparing natural regeneration to active forest restoration. Science Advances 4(5): eaas9143.
Robertson HA, Ausseil A-G, Rance B, Betts H, Pomeroy E 2019. Loss of wetlands since 1990 in Southland, New Zealand. New Zealand Journal of Ecology 43(1): 3355.
Sanderson EW, Jaiteh M, Levy MA, Redford KH, Wannebo AV, Woolmer G 2002. The human footprint and the last

of the wild: the human footprint is a global map of human influence on the land surface, which suggests that human beings are stewards of nature, whether we like it or not. BioScience 52(10): 891–904.

Snelder TH, Biggs BJF 2002. Multiscale river environment classification for water resources management. Journal of the American Water Resources Association 38(5): 1225–1239.

Stats NZ 2023. Statistical standard for geographic areas 2023 (updated December 2023). Stats NZ Tatauranga Aotearoa. 45p.

Sullivan JJ, Williams PA, Timmins SM, Smale MC 2009. Distribution and spread of environmental weeds along New Zealand roadsides. New Zealand Journal of Ecology 33(2): 190–204.

Tulloch VJ, Tulloch AI, Visconti P, Halpern BS, Watson JE, Evans MC, Auerbach NA, Barnes M, Beger M, Chadès I, Giakoumi S, McDonald-Madden E, Murray NJ, Ringma J, Possingham HP 2015. Why do we map threats? Linking threat mapping with actions to make better conservation decisions. Frontiers in Ecology and the Environment 13(2): 91–99.

Venter O, Sanderson EW, Magrach A, Allan JR, Beher J, Jones KR, Possingham HP, Laurance WF, Wood P, Fekete BM, Levy MA, Watson JEM 2016a. Sixteen years of change in the global terrestrial human footprint and implications for biodiversity conservation. Nature Communications 7(1): 12558.

Venter O, Sanderson EW, Magrach A, Allan JR, Beher J, Jones KR, Possingham HP, Laurance WF, Wood P, Fekete BM, Levy MA, Watson JEM 2016b. Global terrestrial human footprint maps for 1993 and 2009. Scientific Data 3(1): 160067.

Viles RL, Rosier DJ 2001. How to use roads in the creation of greenways: case studies in three New Zealand landscapes. Landscape and Urban Planning 55(1): 15–27.

Vimal R, Navarro LM, Jones Y, Wolf F, Le Moguédec G, Réjou-Méchain M 2021. The global distribution of protected areas management strategies and their complementarity for biodiversity conservation. Biological Conservation 256: 109014.

Whitehead AL, Booker DJ 2020. NZ river maps: an interactive online tool for mapping predicted freshwater variables across New Zealand. Christchurch, NIWA. https://niwa.co.nz/freshwater/new-zealand-river-maps (accessed 1 July 2024).

Williams BA, Venter O, Allan JR, Atkinson SC, Rehbein JA, Ward M, Di Marco M, Grantham HS, Ervin J, Goetz SJ, Hansen AJ, Jantz P, Pillay R, Rodríguez-Buriticá S, Supples C, Virnig ALS, Watson JEM 2020. Change in terrestrial human footprint drives continued loss of intact ecosystems. One Earth 3(3): 371–382.

Woolmer G, Trombulak SC, Ray JC, Doran PJ, Anderson MG, Baldwin RF, Morgan A, Sanderson EW 2008. Rescaling the human footprint: a tool for conservation planning at an ecoregional scale. Landscape and Urban Planning 87(1): 42–53.

Received: 5 March 2024; accepted: 17 October 2024
Editorial board member: Zachary Carter

Supplementary material

Additional supporting information may be found in the supplementary material file for this article:

Appendix S1. Difference between the local layers (2012 and 2018).

The New Zealand Journal of Ecology provides supporting information supplied by the authors where this may assist readers. Such materials are peer-reviewed but any issues relating to this information (other than missing files) should be addressed to the authors.